Quantum oscillation of thermally activated conductivity in a monolayer math xmlns="http://www.w3.org/1998/Math/MathML">msub>mrow>mi>WTe/mi>/mrow>mn>2/mn>/msub>/math>-like excitonic insulator

Wen-Yu He and Patrick A. Lee

Phys. Rev. B **104**, L041110 — Published 23 July 2021

DOI: 10.1103/PhysRevB.104.L041110

Quantum Oscillation of Thermally Activated Conductivity in a Monolayer WTe_2-like Excitonic Insulator

Wen-Yu He and Patrick A. Lee*
Department of Physics, Massachusetts Institute of Technology, Cambridge, Massachusetts 02139, USA
(Dated: July 9, 2021)

Recently, quantum oscillation of the resistance in insulating monolayer WTe_2 was reported. An explanation in terms of gap modulation in the hybridized Landau levels of an excitonic insulator was also proposed by one of us. However, the previous picture of gap modulation in the Landau levels spectrum was built on a pair of well nested electron and hole Fermi surfaces, while the monolayer WTe_2 has one hole and two electron Fermi pockets with relative anisotropy. Here we demonstrate that for system like monolayer WTe_2, the excitonic insulating state arising from the coupled one hole and two electron pockets possesses a finite region in interaction parameter space that shows gap modulation in a magnetic field. In this region, the thermally activated conductivity displays the $1/B$ periodic oscillation and it can further develop into discrete peaks at low temperature, in agreement with the experimental observation. We show that the relative anisotropy of the bands is a key parameter and the quantum oscillations decrease rapidly if the anisotropy increases further than the realistic value for monolayer WTe_2.

Introduction. Monolayer WTe_2 is a two-dimensional crystal that exhibits many unusual properties: it is a quantum spin Hall insulator up to relatively high temperature and is a superconductor when doped [1–6]. Recently, quantum oscillation (QO) of the resistance was reported in monolayer WTe_2 when it is gate tuned to be an insulator [7]. In a separate paper, it was argued that the insulating state of monolayer WTe_2 is an excitonic insulator [8]. These observations in monolayer WTe_2 put it into the category of the insulators like SmB_6 [9] and YbB_{12} [10], which possess QOs along with insulating electrical conductivity. As the canonical understanding of QOs is based on the existence of electron Fermi surface (FS) in materials [11], the origin of QO observed in the insulating monolayer WTe_2 requires an explanation.

The paradox of QO in the insulating monolayer WTe_2 without electron FS has inspired suggestions of neutral FS existing inside the insulating gap, where the neutral FS is formed from itinerant spinons that result from the spin-charge separation of holes [7]. The neutral FS hypothesis requires the electronic correlation in monolayer WTe_2 to be strong enough to fractionalize the holes into spinons and holons [12–14]. On the other hand, a more conventional but still nontrivial explanation that does not appeal to strong electronic correlation in monolayer WTe_2 was proposed by one of us: the observed QO of resistance can arise from a small modulation of the insulating gap induced by magnetic field [15]. In the phenomenological model, the gap modulation can give rise to oscillation of thermally activated conductivity and the oscillation further evolves into sharp periodic spikes in low temperature [15], which matches qualitatively well with the temperature dependent behavior of conductance oscillation in monolayer WTe_2. In monolayer WTe_2 the bandwidth is not particularly narrow and strong electronic correlation is not expected in this material; so the modulation of excitonic insulating gap by magnetic field is an attractive alternative explanation for the QO in the insulating monolayer WTe_2. Since the origin of QO reported in WTe_2 is still under debate, we will proceed with further analysis of the gap modulation model, which is an interesting theoretical problem in its own right.

The scenario of magnetic field modulated insulating gap was first proposed to explain the QO of magnetization observed in the Kondo insulator SmB_6 [16–18], and later it successfully predicted the QO of conductance in the inverted narrow gap regime of InAs/GaSb quantum wells [19–21]. In both SmB_6 and InAs/GaSb quantum wells, the insulating gap arises from the hybridization of a single electron band which overlaps a single hole band. Since both are assumed to be isotropic, the system is perfectly nested and fully gapped by the hybridization. Prior to hybridization, the Landau levels in the presence of a magnetic field B moves up in energy in the electron band and down in the hole band. These collide in a periodic way as a function of $1/B$. The memory of this periodicity is retained in the energy gap after hybridization, leading to a periodic modulation of the hybridization gap [16–19]. However, in the case of monolayer WTe_2, there are one hole and two electron Fermi pockets with relative anisotropy [1, 8, 22–24], and in general these pockets are not well nested. The distinctive type of band structure of monolayer WTe_2 shown in Fig. 1 complicates the application of the gap modulation scenario, raising the question of whether QO oscillations survive in the case of the coupled three Fermi pockets in monolayer WTe_2.

In this work, we show that for a monolayer WTe_2-like excitonic insulator, there exists a reasonable range of parameter space which exhibits QO of thermally activated conductivity that originates from the magnetic field induced gap modulation. In the excitonic insulating state, the two electron pockets are first shifted to the middle hole pocket and the mutual couplings among the three Fermi pockets gap out the FSs. Suppose V_1 is the cou-

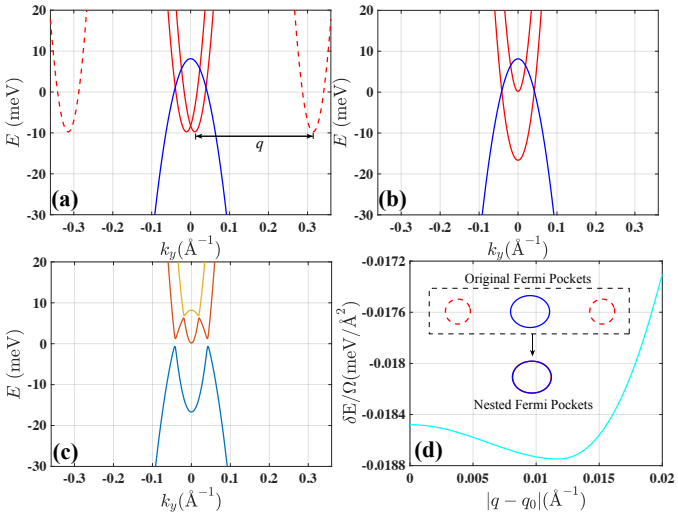

FIG. 1: (a) Band structure of monolayer WTe_2. The red dashed lines denote the original position of conduction bands. Due to the density modulation in the excitonic insulating state, the original conduction bands are shifted to $\boldsymbol{k}=\mathbf{0}$ by $\pm\boldsymbol{q}$. (b) The energy dispersions when the two conduction bands in (a) have finite hybridization V_2 but no coupling ($V_1=0$) with the valence band. They are split into upper and lower bands. (c) The insulating gap generated from (b) by setting the coupling $V_1\neq 0$. (d) The energy density gained in the insulating state as a function of the deviation of q from q_0. Here Ω is the sample area and the energy gained is $\delta E=\langle E\rangle-\langle E\rangle_0$ with $\langle E\rangle_0$ being the ground state energy at $(V_1,V_2)=(0,0)$ meV. The inset inside the dashed rectangle shows the original electron and hole Fermi pockets. At the optimal shift momentum $\boldsymbol{q}$ with $V_2=-7.9$ meV, the electronic pocket from lower band in (b) gets well nested with the hole pocket. In the calculations the chemical potentials are taken to be $\mu_c=9.7$ meV and $\mu_v=8.1$ meV.

pling between the electron and hole pockets and V_2 is the hybridization between the two electronic pockets, the system will self-tune to the optimal shift momentum $\pm\boldsymbol{q}$ that minimizes the ground state energy. Note that in general $\boldsymbol{q}$ is different from $\boldsymbol{q_0}$ which is the separation between the top of the hole band and the bottom of the conduction band. We first minimize the energy with respect to the shift vector $|\boldsymbol{q}|$, and then construct the phase diagram in the parameter space of (V_1,V_2). We find that the insulating regime has the "<" shape looking, and near the tip area of "<" the insulating gap has reasonable modulation (see Fig. 2 and 3). We find that the area in the phase diagram that can generate finite gap modulation depends on the relative anisotropy of Fermi pockets: it shrinks as the relative anisotropy increases. For the monolayer WTe_2 with the relative anisotropy estimated to be around 1.5 [24], we find that the gap modulation near the tip area of "<" can indeed give rise to observable conductivity oscillation (see Fig. 3 and 4), so it gives the possibility that the gap modulation scenario can explain the QO in monolayer WTe_2.

Model for the excitonic insulating state. The monolayer WTe_2 has a hole Fermi pocket centered at $\boldsymbol{k}=\mathbf{0}$ and two flanking electronic Fermi pockets at $\boldsymbol{k}=\pm\boldsymbol{q}_0$ with $\boldsymbol{q}_0=(0,q_0)$, as is shown in the inset of Fig. 1 (d). In the band basis, the quadratic dispersions are taken to approximate the conduction band as $\epsilon_{\pm}(\boldsymbol{k})\approx\frac{\hbar^2k_x^2}{2m_{c,x}}+\frac{\hbar^2(k_y\mp q_0)^2}{2m_{c,y}}-\mu_c$, and also the valence band as $\epsilon_v(\boldsymbol{k})\approx-\frac{\hbar^2k_x^2}{2m_{v,x}}-\frac{\hbar^2k_y^2}{2m_{v,y}}+\mu_v$. The band masses are fit to be $m_{c,x}=m_{c,y}=0.29m_e$, $m_{v,x}=\frac{2}{3}m_{v,y}=0.56m_e$ [24]. Here the relative anisotropy of the electron and hole pockets is controlled by $\gamma=\frac{m_{v,y}m_{c,x}}{m_{v,x}m_{c,y}}$. Note that since it is always possible to rescale the k_y axis so that one of the the bands is isotropic, even in the presence of a magnetic field, it is only the relatively anisotropy that matters in the discussion that follows. When the Coulomb interaction effect is neglected, the conduction band stays at its original position as is indicated by the red dashed line in Fig. 1 (a).

The role of Coulomb interaction in the system with energy overlap between the conduction and valence bands is to provide an effective inter-band attraction to bind electrons and hole states into excitons [25–28]. In an excitonic insulator, a density modulation at $\boldsymbol{q}$ is spontaneously generated, so the original electron and hole Fermi pockets are shifted to gap out the entire FS. For the monolayer WTe_2 type of band structure which has two conduction band minima and one valence band maximum, besides the coupling between the conduction and valence bands, the hybridization between the two electron pockets is also needed to generate the insulating gap [15]. As a result, the generic mean field Hamiltonian matrix for the excitonic insulating state is assumed to have the form

$$H=\begin{pmatrix}\epsilon_v(\boldsymbol{k}) & V_1 & V_1\\ V_1 & \epsilon_+(\boldsymbol{k}+\boldsymbol{q}) & V_2\\ V_1 & V_2 & \epsilon_-(\boldsymbol{k}-\boldsymbol{q})\end{pmatrix}, \qquad (1)$$

where the basis is $[\psi_{v,\boldsymbol{k}},\psi_{+,\boldsymbol{k}+\boldsymbol{q}},\psi_{-,\boldsymbol{k}-\boldsymbol{q}}]^T$ with $\psi_{v,\boldsymbol{k}}$, $\psi_{\pm,\boldsymbol{k}}$ to annihilate a state at $\boldsymbol{k}$ in the valence and conduction bands respectively. Here the coupling potential V_1 is from the pseudo-spin density order at $\boldsymbol{q}$ while the hybridization V_2 comes from the charge density order at $2\boldsymbol{q}$, which can be obtained from the Hartree-Fock mean field calculation [29]. The pseudo-spin index is dropped as it does not affect the energy eigenvalue [30]. Due to the spontaneous generated density order, the original conduction bands are first shifted to $\boldsymbol{k}=\mathbf{0}$ as is seen in Fig. 1 (a). Then the potential V_2 hybridizes the two conduction bands, generating two new conduction bands with different energies shown in Fig. 1 (b). We refer to these as the upper and lower bands. Finally, the valence band couples with the two new conduction bands individually and an excitonic insulating gap appears in Fig. 1 (c). Importantly, for negative V_2 the coupling between the valence band and the lower conduction band is dominant

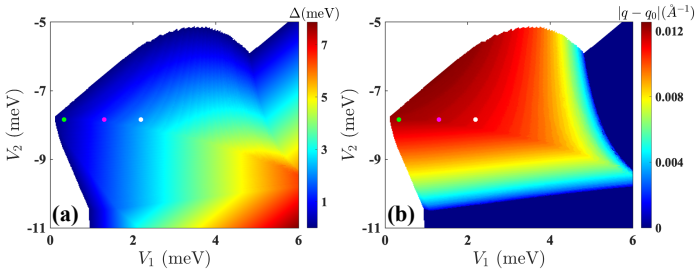

FIG. 2: The insulating phase diagram of a monolayer WTe_2-like excitonic insulator using realistic band parameters which sets the relative anisotropy to be $\gamma = 1.5$. At given coupling potential (V_1, V_2), the gap size Δ is given in (a) and the associated shift momentum $|q - q_0|$ is present in (b).

in the insulating gap generation [30] while for positive V_2 it is the opposite. Clearly negative V_2 is preferable for energy gain and our calculations are mainly in this domain. Since a microscopic model for the interaction parameters is not known, in this paper we do not attempt to perform a self-consistent calculation starting with a microscopic model, but consider only the parameter space controlled by the mean field parameters V_1 and V_2.

For a given V_1 and V_2 , the system will self-tune to have the ground state energy $\langle E\rangle = \sum_{\boldsymbol{k},\nu} f\left[E_\nu\left(\boldsymbol{k}\right)\right] E_\nu\left(\boldsymbol{k}\right)$ minimized by varying the shift momentum $\boldsymbol{q} = (0, q)$. Here $f\left(\epsilon\right)$ is the Fermi Dirac distribution function and $E_\nu\left(\boldsymbol{k}\right)$ with $\nu = 1, 2, 3$ is the energy eigenvalue of the Hamiltonian H in Eq. 1. In the simple case when there is no relative anisotropy ($\gamma = 1$), for sufficient large V_2 the ground state energy gets minimized at $\boldsymbol{q} = \boldsymbol{q}_0$ when only the electron pocket corresponding to the lower band crosses the Fermi level and is perfectly nested with the hole pocket [30]. In the realistic monolayer WTe_2 band structure, the middle hole pocket is more elliptical than the flanking electron pockets, so it is no longer true that the optimal nesting always occurs at $\boldsymbol{q} = \boldsymbol{q}_0$. Instead the $\boldsymbol{q}$ may be adjusted so that one side of the electron pocket has optimal overlap with a side of the hole pocket. In Fig. 1 (d), the energy density gained in the insulating state is plotted as a function of $|\boldsymbol{q}-\boldsymbol{q}_0|$ with $(V_1, V_2) = (1.3, -7.9)$ meV, which shows that the ground state energy takes the minimal value at nonzero $|\boldsymbol{q} - \boldsymbol{q}_0|$. By calculating the insulating gap size and the associated shift momentum $\boldsymbol{q}$ in a range of the coupling potentials V_1, V_2, the excitonic insulating phase diagram in terms of (V_1, V_2) is obtained in Fig. 2 using realistic parameters for monolayer WTe_2. In the phase diagram, the gapped regime has a pointy "<" shape, and the finite $|\boldsymbol{q} - \boldsymbol{q}_0|$ near the tip of "<" makes the V_2 hybridized electronic pockets well nested with the middle hole pocket as can be seen in the inset of Fig. 1 (d). As we shall see, it is in this well nested region that the gap modulation and QO in the presence of a magnetic field survives the best.

Gap modulation in the Landau levels spectrum. In the presence of magnetic field, the original quadratic energy dispersions for the conduction and valence bands form three sets of Landau levels: $\epsilon_{\pm,n} = \left(n + \frac{1}{2}\right)\hbar\omega_{\rm c} - \mu_{\rm c}$, $\epsilon_{{\rm v},n} = -\left(n + \frac{1}{2}\right)\hbar\omega_{\rm v} + \mu_{\rm v}$, with $n \in \mathbb{Z}$. Here the cyclotron frequencies are $\omega_{\rm c} = \frac{eB}{m_{\rm c}}$, $\omega_{\rm v} = \frac{eB}{m_{\rm v}}$, with the cyclotron masses being $m_{\rm c} = \sqrt{m_{{\rm c},x} m_{{\rm c},y}}$, $m_{\rm v} = \sqrt{m_{{\rm v},x} m_{{\rm v},y}}$. In the excitonic insulating state, due to the couplings among the original conduction and valence bands, the formed Landau levels get hybridized, resulting in an insulating gap as a function of magnetic field B. The Hamiltonian matrix that involves Landau levels hybridizations has similar form as that in Eq. 1 [30]

$$\hat{H} = \begin{pmatrix} \hat{H}_{\rm v} & \hat{V}_1 & \hat{V}_1 \\ \hat{V}_1^\dagger & \hat{H}_+ & \hat{V}_2 \\ \hat{V}_1^\dagger & \hat{V}_2^\dagger & \hat{H}_- \end{pmatrix}, \tag{2}$$

where the matrix elements are given in Landau gauge $\boldsymbol{A} = (0, Bx, 0)$ as

$$\hat{H}_{{\rm v},n,m} = \langle {\rm v}, n| - \frac{1}{2}\hbar\omega_{\rm v}\left(a_{\rm v}^\dagger a_{\rm v} + a_{\rm v} a_{\rm v}^\dagger\right) + \mu_{\rm v}\left|{\rm v}, m\right\rangle, \tag{3}$$

$$\hat{H}_{\pm,n,m} = \langle {\rm c}, n|\, \frac{1}{2}\hbar\omega_{\rm c}\left\{\left[a_{\rm c}^\dagger \mp \frac{l_{{\rm c},B}}{\sqrt{2}}\left(q - q_0\right)\right]\left[a_{\rm c} \mp \frac{l_{{\rm c},B}}{\sqrt{2}}\left(q - q_0\right)\right] + \left[a_{\rm c} \mp \frac{l_{{\rm c},B}}{\sqrt{2}}\left(q - q_0\right)\right]\left[a_{\rm c}^\dagger \mp \frac{l_{{\rm c},B}}{\sqrt{2}}\left(q - q_0\right)\right]\right\} - \mu_{\rm c}\left|{\rm c}, m\right\rangle, \tag{4}$$

$$\hat{V}_{1,n,m} = \langle {\rm v}, n|\, V_1\left|{\rm c}, m\right\rangle, \quad \text{and} \quad \hat{V}_{2,n,m} = \langle {\rm c}, n|\, V_2\left|{\rm c}, m\right\rangle, \tag{5}$$

with $l_{{\rm c},B} = \sqrt{\frac{\hbar}{m_{{\rm c},x}\omega_{\rm c}}}$. Here the basis $\left|{\rm v}, n\right\rangle = \frac{\left(a_{\rm v}^\dagger\right)^n}{\sqrt{n!}}\left|{\rm v}, 0\right\rangle$ and $\left|{\rm c}, n\right\rangle = \frac{\left(a_{\rm c}^\dagger\right)^n}{\sqrt{n!}}\left|{\rm c}, 0\right\rangle$ are the eigenstates corresponding to the nth Landau level from the valence band $\epsilon_{\rm v}\left(\boldsymbol{k}\right)$ and the $\boldsymbol{k} = \boldsymbol{0}$ centered conduction band $\epsilon_{\rm c}\left(\boldsymbol{k}\right) = \frac{\hbar^2 k_x^2}{2m_{{\rm c},x}} + \frac{\hbar^2 k_y^2}{2m_{{\rm c},y}} - \mu_{\rm c}$ respectively. It is clear that $\hat{H}_{\rm v}$ and $\hat{H}_\pm$ gives energy eigenvalues $\epsilon_{{\rm v},n}$ and $\epsilon_{\pm,n}$ respectively. Suppose the FS area covered by the electron pockets and hole pocket are both equivalent to S, which is required by charge neutrality, then the chemical potentials for the

original conduction and valence bands are solved to be $\mu_c = \frac{\hbar^2 S}{4\pi m_c}$, $\mu_v = \frac{\hbar^2 S}{2\pi m_v}$. It indicates that once the cyclotron masses m_c, m_v and the FS area S are fixed, the energy eigenvalue of the Hamiltonian in Eq. 2 depends only on the specific forms of the hybridization matrix $\hat{V}_1$, $\hat{V}_2$. In the case that Fermi pockets have no relative anisotropy ($\gamma = 1$), the hybridization matrix $\hat{V}_1$, $\hat{V}_2$ are both diagonal, so the energy eigenvalue are analytically solved to be [30]

$$E_{1,n} = \frac{1}{2}\left(\tilde{\epsilon}_{c,n} + \epsilon_{v,n}\right) + \sqrt{\frac{1}{4}\left(\tilde{\epsilon}_{c,n} - \epsilon_{v,n}\right)^2 + 2V_1^2}, \quad (6)$$

$$E_{2,n} = \frac{1}{2}\left(\tilde{\epsilon}_{c,n} + \epsilon_{v,n}\right) - \sqrt{\frac{1}{4}\left(\tilde{\epsilon}_{c,n} - \epsilon_{v,n}\right)^2 + 2V_1^2}, \quad (7)$$

$$E_{3,n} = \hbar\omega_c\left(n + \frac{1}{2}\right) - V_2, \quad (8)$$

with $\tilde{\epsilon}_{c,n} = \hbar\omega_c\left(n + \frac{1}{2}\right) + V_2$. The resulting Landau levels spectrum always have the magnetic field modulated gap $\sqrt{\left(\tilde{\epsilon}_{c,n} - \epsilon_{v,n}\right)^2 + 8V_1^2}$ and the modulation periodicity is determined by the FS area before hybridization [16, 30]. In the more general case of monolayer WTe_2 type band structure that has relative anisotropy $\gamma > 1$, the off-diagonal elements in the hybridization matrix $\hat{V}_1$ are generally nonzero (the detailed calculations for the matrix elements of $\hat{V}_1$ are present in the Supplemental Material [30]). As numerically diagonalizing $\hat{H}$ gives the the hybridized Landau levels spectrum in the case of $\gamma > 1$, the effect of relative anisotropy on the magnetic field induced gap modulation can be figured out.

For the monolayer WTe_2, the electron and hole cyclotron masses take the value $m_c = 0.29m_e$, $m_v = 0.67m_e$ [24]. Given the experimental observed QO frequency $f = 48.6$ T in device 1 [7], the FS area S can be determined by the Onsager theorem $f = \frac{\hbar S}{2\pi e}$, so the chemical potentials are fixed to be $\mu_c = 9.7$ meV, $\mu_v = 8.1$ meV. The set of parameters m_c, m_e, μ_c and μ_v along with the relative anisotropy $\gamma = 1.5$ have been applied in the calculation for the phase diagram present in Fig. 2. Three points with the same V_2 but different V_1 in the phase diagram are selected to calculate the Landau levels spectrum. The Landau levels spectrum from the green, magenta, and white colored phase points in Fig. 2 are plotted as a function of $1/B$ in Fig. 3 (a), (b) and (c) respectively. The hybridization of Landau levels described by Eq. 2 inherits the feature of the three bands coupling in Eq. 1. The hybridization matrix $\hat{V}_2$ first lifts the degeneracy of $\epsilon_{\pm,n}$, giving two sets of Landau levels that are from the two new conduction bands in Fig. 1 (b). Then the newly generated two sets of Landau levels couple individually with the valence band Landau levels $\epsilon_{v,n}$, eventually generating the gap in the Landau levels spectrum. In Fig. 3 (a), with given (V_1, V_2) near the tip of the gapped region, the gap in the Landau levels spectrum shows significant modulation in the magnetic field.

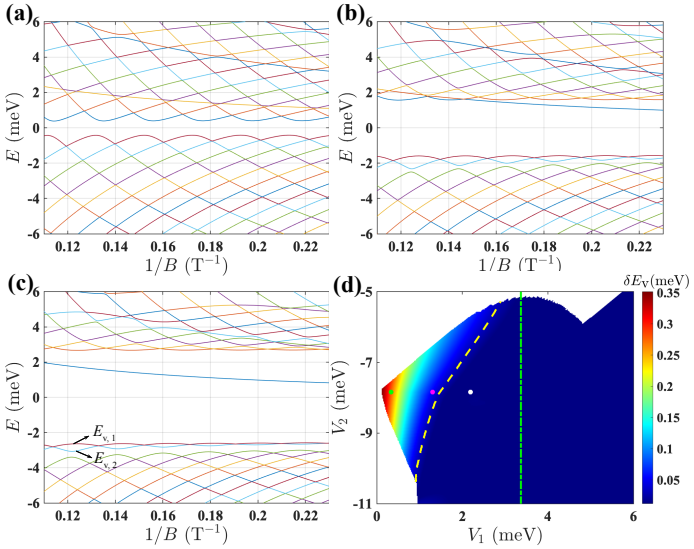

FIG. 3: The Landau levels spectrum from the green, magenta and white phase points in Fig. 2 for (a), (b) and (c) respectively. Notice that a band which corresponds to the upper electron band in Fig. 1 (b) is very weakly hybridized and stays at the same energy. It moves inside the gap when the gap opens for increasing V_1. It shows no modulation with B. On the other hand, the top of the valence band always shows modulations, even though it is weakened for increasing V_1. (d) The gap modulation of the valence band is characterized by the energy difference δE_v at given (V_1, V_2) in the gapped region. The yellow dashed line is the contour of $\delta E_v = 0.03$ meV. Recall that the relative anisotropy is $\gamma = 1.5$. For comparison, the green dash-dot line gives the boundary of the region with gap modulation larger than 0.03 meV in $\gamma = 1$ case.

When the coupling potential V_1 increases, the insulating gap becomes larger so the lowest Landau level from the upper conduction band in Fig. 1 (b) appears inside the gap at small B. Since that Landau level has negligible coupling with the valence band Landau levels $\epsilon_{v,n}$, the energy oscillation in the upper boundary of the gap disappears there. On the other hand, the energy oscillation in the lower boundary of the gap survives in the whole range of magnetic field $1/B \in [0.11, 0.23]$ T^{-1} shown in Fig. 3 (b), although it is suppressed a bit due to larger V_1. As the coupling potential V_1 further increases, the energy oscillation in the lower boundary gradually gets smoothed in $1/B > 0.22$ T^{-1} as is shown in Fig. 3 (c).

The energy difference between the top two valence band Landau levels at $E_{v,1}$, $E_{v,2}$ serves as an indicator of the gap modulation. For the Landau levels spectrum in the range of magnetic field $1/B \in [0.11, 0.23]$ T^{-1}, the energy difference $\delta E_v = \frac{1}{2}\left[E_{v,1}(1/B) - E_{v,2}(1/B)\right]$ at $1/B = 0.23$ T^{-1} is calculated in the gapped region, which is shown in Fig. 3 (d). Importantly, the energy difference δE_v is found to decrease from a finite value to zero as (V_1, V_2) goes away from the tip area of "<", and the gap modulation decays in the same way. In Fig. 3

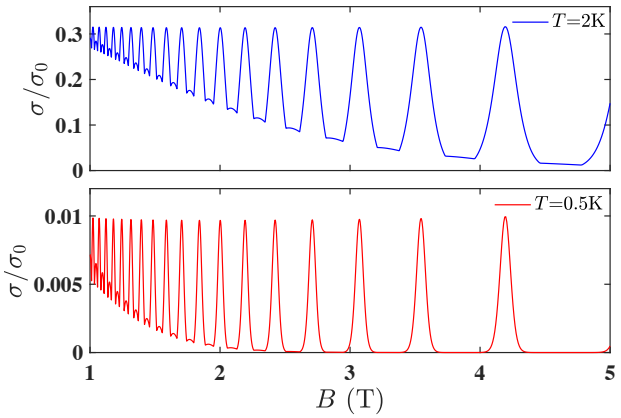

FIG. 4: The thermally activated conductivity calculated from Eq. 9. In the calculation the chemical potentials are fixed to be $\mu_c = 4.6$ meV, $\mu_v = 3.9$ meV so that the Fermi surface area gives the frequency $f = \frac{\hbar S}{2\pi e} = 23$ T.

(d), the contour of $\delta E_v = 0.03$ meV gives an estimate of the regime that has reasonable gap modulation, and the gap modulation is further confirmed by Landau levels spectrum calculations from more points inside the regime $\delta E_v > 0.03$ meV [30]. Compared to the $\gamma = 1$ case where the $V_1 < 3.4$ meV delimits the area of gap modulation larger than 0.03 meV [30], the relative anisotropy $\gamma = 1.5$ reduces the area in the phase diagram. Besides the specific case of $\gamma = 1.5$, the energy difference δE_v in the phase diagram has been calculated for a series of insulating states with $\gamma = 2, 2.5, 3$ in the Supplemental Material [30]. The area with reasonable gap modulation is found to shrink toward the tip of "<" as the relative anisotropy increases. The reason is that as γ increases, the region in parameter space where the electron and hole Fermi surfaces are well nested prior to hybridization by V_1 shrinks. When the Fermi surfaces are not well nested, each Landau level in the hole band is coupled to several other ones in the conduction bands when the magnetic field is turned on, and the gap modulation decreases. Nevertheless, up to $\gamma = 3$, a range of phase space always exists to give gap modulation in the order of 0.1 meV at $1/B = 0.23$ T^{-1}, which is enough to generate QO of thermally activity in the range of magnetic field $B \in [3, 10]$ T [30].

Thermally activated conductivity oscillation. In the excitonic insulating state which occurs at the charge neutrality, the chemical potential always stays inside the hybridization gap, so the charge carriers at finite temperature are the thermally activated electronic states that come from the Landau levels below the gap. The activated conductivity is described by the Arrhenius type equation [31, 32]:

$$\sigma = \sigma_0 \exp\left[-\frac{\Delta(B) - \Delta(0)}{k_b T}\right], \tag{9}$$

where $\Delta(B)$ is the gap at B, and k_b is the Boltzmann constant. Here the prefactor σ_0 is assumed to be independent of B as the chemical potential pinned inside the hybridization gap does not oscillate with the applied magnetic field. In the Landau levels spectrum of a monolayer WTe_2-like excitonic insulator, since the gap $\Delta(B)$ is periodically modulated by the magnetic field B in a range of phase space, the associated thermally activated conductivity also exhibits periodic oscillation in $1/B$. In Fig. 4, the thermally activated conductivity is calculated using the Landau levels spectrum that has periodic gap modulation with the same frequency as observed in the conductance oscillation in device 2 in experiment [7]. As the ratio of conductance between $T = 2$ K and $T = 0.5$ K in device 2 is smaller than 10^2, the gap estimated from Eq. 9 has the upper limit at the order of 0.2 meV. Hence we take the coupling potentials in the Landau levels spectrum to be $(V_1, V_2) = (0.1, 3.7)$ meV so that the Landau levels hybridization gap is around 0.2 meV. The resulting conductivity in Fig. 4 clearly shows the oscillation. At the lower temperature $T = 0.5$ K, the conductivity oscillation evolves into periodic spikes that resembles the discrete peaks observed in the quantized regime in experiment. It matches the fact that lowering temperature makes the quantized regime accessible to the range of magnetic field applied in experiment. In the Supplemental Material [30], thermally activated conductivity has been considered in a range of parameters and the conductivity oscillation is found to be a general phenomenon that will occur in the phase space with visible gap modulation.

Discussion and Summary. In the above sections, the effect of impurities that are always contained in the sample has yet been analyzed, but the scenario of QO from the gap modulation would be the same given the impurity potentials are weak. We know that impurities will lift the degeneracy of each Landau level so that the resulting Landau levels get broadened. Prior to the excitonic hybridization, the broadened Landau levels form peaks in the density of states consisting of extended states, while the states between the peaks are localized. When the excitonic hybridization is turned on, the extended states from the electron band would couple with the extended states in the hole bands to form new extended states. The localized states will also hybridize but remain localized. The resulting hybridized Landau levels in the excitonic insulating state are therefore also broadened in the same way, with extended and localized states. As long as the broadening is smaller than the Landau level spacing, the conductivity from the thermally excited extended states will oscillate due to the gap modulation.

To summarize, for a monolayer excitonic insulator that has one hole and two electronic Fermi pockets similar to that of WTe_2, there exists a range of phase space that can generate QO of thermally activated conductivity. The size of the phase space with finite QO depends on the

relative anisotropy of the Fermi pockets before hybridization. For a relative anisotropy γ estimated up to 3, our study shows that the gap modulation survives near the tip of the gapped region in phase diagram. Since the mean field parameters V_1, V_2 in the phase diagram depends on details of interactions, we do not know whether a self-consistent calculation starting from the electron interactions in the monolayer WTe_2 will land us in that region. Thus while it is possible that the gap modulation scenario can explain the QO observed in monolayer WTe_2, it is not guaranteed to be always the case.

Acknowledgements. The authors acknowledge the support by DOE office of Basic Sciences grant number DE-FG02-03-ER46076.

* palee@mit.edu

[1] X. Qian, J. Liu, L. Fu, and J. Li, Science **346**, 1344 (2014).
[2] S. Tang, C. Zhang, D. Wong, Z. Pedramrazi, H.-Z. Tsai, C. Jia, B. Moritz, M. Claassen, H. Ryu, S. Kahn, J. Jiang, H. Yan, M. Hashimoto, D. Lu, R. G. Moore, C.-C. Hwang, C. Hwang, Z. Hussain, Y. Chen, M. M. Ugea, Z. Liu, X. Xie, T. P. Devereaux, M. F. Crommie, S.-K. Mo, Z.-X. Shen, Nat. Phys. **13**, 683 (2017).
[3] Z. Fei, T. Palomaki, S. Wu, W. Zhao, X. Cai, B. Sun, P. Nguyen, J. Finney, X. Xu, and D. H. Cobden, Nat. Phys. **13**, 677 (2017).
[4] S. Wu, V. Fatemi, Q. D. Gibson, K. Watanabe, T. Taniguchi, R. J. Cava, and P. Jarillo-Herrero, Science **359**, 76 (2018).
[5] V. Fatemi, S. Wu, Y. Cao, L. Bretheau, Q. D. Gibson, K. Watanabe, T. Tanighchi, R. J. Cava, and P. Jarillo-Herrero, Science **362**, 926 (2018).
[6] E. Sajadi, T. Palomaki, Z. Fei, W. Zhao, P. Bement, C. Olsen, S. Luescher, X. Xu, J. A. Folk, and D. H. Cobden, Science **362**, 922 (2018).
[7] P. Wang, G. Yu, Y. Jia, M. Onyszczak, F. A. Cevallos, S. Lei, S. Klemenz, K. Watanabe, T. Taniguchi, R. J. Cava, L. M. Schoop, S. Wu, Nature **589**, 225 (2021).
[8] Y. Jia, P. Wang, C.-L. Chiu, Z. Song, G. Yu, B. Jack, S. Lei, S. Klemenz, F. A. Cevallos, M. Onyszczak, N. Fishchenko, X. Liu, G. Farahi, F. Xie, Y. Xu, K. Watanabe, T. Taniguchi, B. A. Bernevig, R. J. Cava, L. M. Schoop, A. Yazdani, S. Wu, arXiv:2010.05390 (2020).
[9] B. S. Tan, Y.-T. Hsu, B. Zeng, M. C. Hatnean, N. Harrison, Z. Zhu, M. Hartstein, M.Kiourlappou, A. Srivastava, M. D. Johannes, T. PT. Murphy, J.-H. Park, L. Balicas, G. G. Lonzarich, G. Balakrishnan, S. E. Sebastian, Science **349**, 287 (2015).
[10] Z. Xiang, Y. Kasahara, T. Asaba, B. Lawson, C. Tinsman, L. Chen, K. Sugimoto, S. Kawaguchi, Y. Sato, G. Li, S. Yao, Y. L. Chen, F. Lga, J. Singleton, Y. Matsuda, L. Li, Science **362**, 65 (2018).
[11] D. Shoenberg, *Magnetic Oscillations in Metals* (Cambridge University Press, Cambridge, England, 1984).
[12] O. I. Motrunich, Phys. Rev. B **73**, 155115 (2006).
[13] D. Chowdhury, I. Sodemann, and T. Senthil, Nat. Commun. **9**, 1766 (2018).
[14] I. Sodemann, D. Chowdhury, and T. Senthil, Phys. Rev. B **97**, 045152 (2018).
[15] P. A. Lee, Phys. Rev. B **103**, L041101 (2021).
[16] J. Knolle and N. R. Cooper, Phys. Rev. Lett. **115**, 146401 (2015).
[17] L. Zhang, X.-Y. Song, and F. Wang, Phys. Rev. Lett. **116**, 046404 (2016).
[18] J. Knolle and N. R. Cooper, Phys. Rev. Lett. **118**, 096604 (2017).
[19] J. Knolle and N. R. Cooper, Phys. Rev. Lett. **118**, 176801 (2017).
[20] D. Xiao, C.-X. Liu, N. Samarth, and L.-H. Hu, Phys. Rev. Lett. **122**, 186802 (2019).
[21] Z. Han, T. Li, L. Zhang, G. Sullivan, and R.-R. Du, Phys. Rev. Lett. **123**, 126803 (2019).
[22] L. Muechler, A. Alexandradinata, T. Neupert, and R. Car, Phys. Rev. X **6**, 041069 (2016).
[23] L.-k. Shi and J. C. W. Song, Phys. Rev. B **99**, 035403 (2019).
[24] H. Y. Lv, W. J. Lu, D. F. Shao, Y. Liu, S. G. Tan, and Y. P. Sun, Europhys. Lett. **110**, 37004 (2015).
[25] D. Jérome, T. M. Rice, and W. Kohn, Phys. Rev. **158**, 462 (1967).
[26] W. Kohn, Phys. Rev. Lett. **19**, 439 (1967).
[27] B. I. Halperin and T. M. Rice, Rev. Mod. Phys. **40**, 755 (1968).
[28] B. I. Halperin and T. M. Rice, Solid State Phys, **21**, 115 (1968).
[29] Y. H. Kwan, T. Devakul, S. L. Sondhi, S. A. Parameswaran, arXiv:2012.05255 (2020).
[30] See Supplemental Materials for details on 1) the coupling among three bands in the mean field Hamiltonian, 2) the nesting of Fermi pockets in ground state with optimal shift momentum, 3) the calculation of Landau levels coupling matrix elements, and 4) numerical calculation of Landau levels spectrum, thermally activated conductivity in a range of parameter space.
[31] D. G. Polyakov and B. I. Shklovskii, Phys. Rev. Lett. **73**, 1150 (1994).
[32] D. G. Polyakov and B. I. Shklovskii, Phys. Rev. Lett. **74**, 150 (1995).